

Size-dependent photoluminescence from surface-oxidized Si nanocrystals in a weak confinement regime

Shinji Takeoka

Division of Mathematical and Material Science, The Graduate School of Science and Technology, Kobe University, Rokkodai, Nada, Kobe 657-8501, Japan

Minoru Fujii* and Shinji Hayashi

Department of Electrical and Electronics Engineering, Faculty of Engineering, Kobe University, Rokkodai, Nada, Kobe 657-8501, Japan

(Received 1 June 2000; revised manuscript received 2 October 2000)

Photoluminescence (PL) from surface-oxidized Si nanocrystals (nc-Si) was studied as a function of the size. The size of nc-Si was comparable with or larger than the Bohr radius of free excitons in bulk Si crystal (5 nm). In contrast to smaller surface-oxidized nc-Si (typically as small as a few nanometers in diameter), these relatively large nc-Si exhibited PL properties with strong size dependence. A high-energy shift of the PL peak from the vicinity of the bulk band gap to the visible region was observed. This PL shift was accompanied by a shortening of the PL lifetime and an increase in the exchange splitting energy of excitons. These size dependences indicate that the PL originates from the recombination of excitons confined in nc-Si. The differences in the PL properties between H-terminated and surface-oxidized nc-Si are also discussed.

I. INTRODUCTION

Since the observation of the efficient visible photoluminescence (PL) from porous Si,¹ optical properties of Si nanostructures have been the subject of intensive research because they offer a good system to understand zero-dimensional quantum size effects in indirect-gap semiconductors.²⁻⁵ Various types of Si nanostructures have been fabricated so far. They can be classified into two categories based on the surface termination: one is H-terminated Si nanocrystals (nc-Si) (Refs. 6-8) and the other is O-terminated (surface oxidized) nc-Si.⁸⁻²² Fresh porous Si belongs to the first category, while aged or intentionally surface oxidized porous Si belong to the second category. In the second category, nc-Si embedded in SiO₂ thin films are intensively studied. These films are obtained by annealing nonstoichiometric SiO₂ (SiO_x) prepared by Si ion implantation into SiO₂ or cosputtering Si and SiO₂.

In the case of H-terminated fresh porous Si, a continuous shift of the PL peak from the bulk band gap to the visible region has been reported.^{3,5,7} Moreover, shortening of the PL lifetime and increase in the exchange splitting energy of excitons have been reported.^{5,7} All these observed PL properties could be well explained by a quantum confinement model.

In contrast to the wide tunability of the PL energy of fresh porous Si, PL from surface-oxidized nc-Si was in most cases observed in the energy range between 1.4 and 1.8 eV;⁸⁻²² no PL data have been reported between the bulk band gap and 1.4 eV. The lack of the PL data in that range and the small tunability of the PL peak brought about a controversy about the PL mechanism. Besides the quantum confinement model,⁸⁻¹⁷ oxygen-related localized states¹⁸⁻²² and Si-based chemical species models²³ have been proposed as the origin of the PL.

The purpose of this work is to prepare relatively large surface-oxidized nc-Si that show luminescence in the vicinity

of the bulk band gap, i.e., in a weak confinement regime, and clarify their PL properties. We show that the surface-oxidized nc-Si exhibit efficient luminescence at room temperature, and the PL properties are very sensitive to the size. The observed results are compared with those of H-terminated nc-Si, and the effects of the surface termination on the PL properties of nc-Si are discussed.

II. EXPERIMENTAL PROCEDURE

Si nanocrystals embedded in SiO₂ matrices were prepared by an rf cosputtering method. Si and SiO₂ sputtering targets were simultaneously sputtered in Ar gas of 0.5 Pa (background pressure of 5×10^{-6} Pa) using a multitarget sputtering apparatus. The substrates were (100)-oriented Si wafers for infrared absorption measurements and fused-quartz plates for PL measurements. The deposition rate was 10 nm/min, and the thickness of the films was about 300 nm. After the deposition, the films were annealed in an N₂ gas atmosphere to grow nc-Si in SiO₂ matrices. The size of nc-Si was controlled by changing the annealing temperature (T_a) and the volume fraction of nc-Si (f_{Si}). f_{Si} was estimated from infrared absorption spectra.^{11,24}

PL spectra were measured using a single monochromator equipped with an InP/In_xGa_{1-x}As photocathode near-infrared photomultiplier. The excitation source was the 488-nm line of an Ar-ion laser. The excitation power was selected as low as possible (4 mW/cm²). The laser beam was chopped by using an acousto-optic modulator at a frequency of 16 Hz. The spectral response of the detection system was calibrated with the aid of a reference spectrum of a standard tungsten lamp. The PL decay curves were measured by pumping to steady state and chopping the laser with the same frequency as used for the PL measurements.^{9,10} The overall time resolution of the system was about 40 ns. The PL and the PL decay dynamics were measured from 4 to 295 K in a continuous-flow He cryostat.

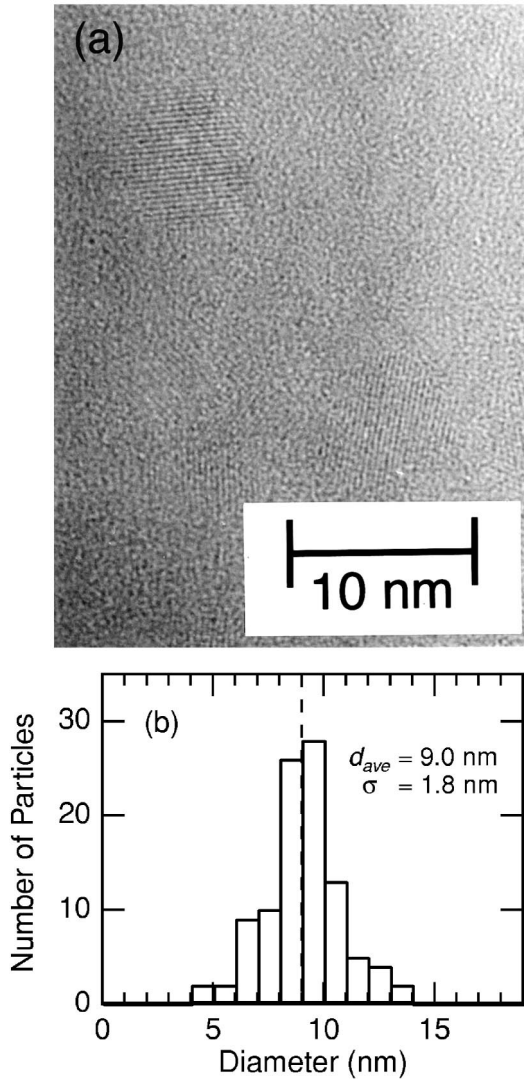


FIG. 1. (a) Cross-sectional HRTEM image of the sample with $f_{\text{Si}}=0.16$ and $T_a=1300^\circ\text{C}$. Lattice fringes corresponding to the $\{111\}$ planes of Si with the diamond structure can clearly be seen. (b) Size distribution of nc-Si in the same sample.

After the optical measurements, the cross sections of the samples were observed by a high-resolution transmission electron microscope (HRTEM). The samples for the HRTEM observations were prepared by standard procedures including mechanical and Ar-ion thinning techniques.

III. RESULTS AND DISCUSSION

A. HRTEM observation

Figure 1(a) shows the cross-sectional HRTEM image for the sample with $f_{\text{Si}}=0.16$ and $T_a=1300^\circ\text{C}$. Lattice fringes corresponding to the $\{111\}$ planes of Si with the diamond structure can clearly be seen. The shape of nc-Si is almost spherical and the crystallinity is very good. Figure 1(b) shows the size distribution obtained from several HRTEM images. The average diameter (d_{av}) and the standard deviation (σ) are 9.0 and 1.8 nm, respectively. The values of d_{av} and σ obtained from five samples are listed in Table I. The size of nc-Si is varied from 4.2 to 9.0 nm, and σ is about 20% of d_{av} for all the samples.

TABLE I. Summary of sample parameters: the annealing temperature (T_a), the volume fraction of nc-Si (f_{Si}), the average diameter of nc-Si (d_{av}), the standard deviation of the size (σ), and the PL peak energy at 4 K (E_{PL}).

T_a ($^\circ\text{C}$)	f_{Si}	d_{av} (nm)	σ (nm)	E_{PL} (eV)
1150	0.13	4.2	0.8	1.47
1150	0.16	4.7	0.9	1.37
1200	0.16	5.4	1.1	1.29
1250	0.16	6.7	1.1	1.21
1300	0.16	9.0	1.8	1.18

The HRTEM image shows that nc-Si are isolated from the others by SiO_2 barriers. The distance between the surfaces of neighboring nc-Si is about 4–5 nm. These thick SiO_2 barriers prevent carrier transport between adjacent nc-Si. The complete isolation of carriers is one of the characteristic features of the present samples. In mesoporous Si, the transport of carriers is possible at relatively high temperatures due to their wirelike shape.²⁵

B. Photoluminescence spectra

Figures 2(a) and 2(b) show the dependence of the PL spectra on d_{av} at room temperature and 4 K, respectively. The PL spectra are normalized at their maximum intensities. The PL intensity was saturated at rather low excitation power. In this work, the excitation power was selected in the range where the PL intensity is proportional to the excitation power. At room temperature, the sample with $d_{\text{av}}=9.0$ nm exhibits PL around 1.19 eV. The peak energy is slightly larger than the band-gap energy of bulk Si crystal (1.12 eV). With decreasing d_{av} from 9.0 to 4.2 nm, the PL peak shifts monotonously to higher energy and reaches 1.42 eV.

Figure 3 shows the PL peak energy at room temperature as a function of the size. The solid circles represent the present results. Previous experimental results for surface-oxidized nc-Si prepared by various methods are also shown, i.e., cosputtering of Si and SiO_2 (\circ),^{11,12} plasma decomposition of silane gas and subsequent oxidation (\times),¹⁴ oxidation of aerosol nc-Si (Δ),¹⁵ and Si ion-implantation into SiO_2 (∇).^{16,17} The band-gap energy of bulk Si crystal is shown by the broken line. We can clearly see that the present results fill the region between the previous results in the visible region and the bulk band gap. It should be stressed here that in spite of the different preparation methods, the PL energy smoothly changes in a wide range as the size of nc-Si changes. The deviation of the data at 7.8 nm (Δ) may be caused by the large size distribution.¹⁵ The present results combined with previous ones demonstrate that the PL energy of surface-oxidized nc-Si varies from the vicinity of the bulk band gap to 1.9 eV with decreasing the size from 9 to 1 nm.

In Fig. 3, the PL peak energy is plotted as a function of the average diameter. This plot is meaningless if the PL intensity depends strongly on the size. However, in the present samples, PL intensity is considered to be almost independent of the size due to the following reason. If PL intensity becomes larger with decreasing size, that of the sample with a smaller average size becomes much larger than that with a larger average size. However, in actual samples, in spite of

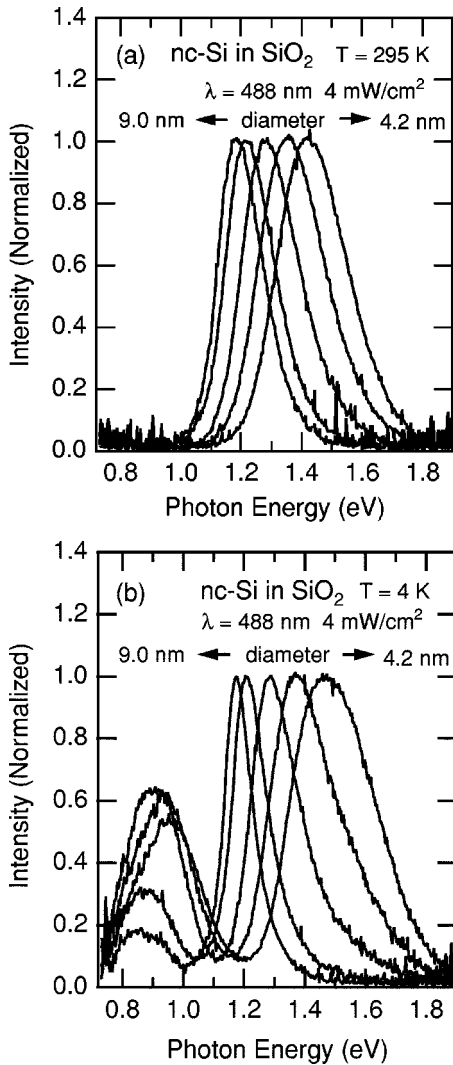


FIG. 2. Dependence of the PL spectra on the average diameter of nc-Si (a) at 295 K and (b) at 4 K.

the strong size dependence of the PL peak energy, PL intensity was almost independent of the average size, meaning that size dependence of the PL intensity is not large. This result and the relatively small size distribution ($\leq 20\%$ of the average diameter) seem to support the validity of the discussion based on the average size.

The situation changes if the excitation power is higher than that used in this work. As will be shown in the next subsection, the PL lifetime at room temperature depends strongly on the size. Since the lifetime becomes longer with increasing size, at high excitation power, PL from larger particles is more easily saturated than that from smaller particles. Therefore, with increasing excitation power, contribution of the smaller particles in the size distribution becomes relatively larger, resulting in the higher-energy shift of the PL peak. In order to avoid these effects, in this work the excitation power was selected in the range where the PL intensity is proportional to the excitation power and the spectral shape does not depend on the excitation power.

Although not shown here, the intensity of the PL was almost independent of the temperature from 4 K to room temperature. This temperature insensitivity may be the characteristic feature of the surface-oxidized nc-Si. The complete

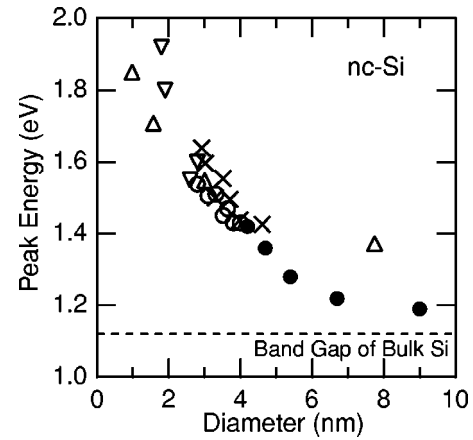


FIG. 3. PL peak energy versus average diameter of nc-Si. Solid circles represent the present results. Previous experimental results are taken from Refs. 11 and 12 (\circ), Ref. 14 (\times), Ref. 15 (\triangle), and Refs. 16 and 17 (∇).

isolation of carriers may be responsible for the high PL efficiency even at room temperature.

At 4 K, in addition to the PL peak around 1.2–1.4 eV, another peak appears around 0.8–0.9 eV [Fig. 2(b)]. The low-energy peak position shows size dependence similar to the high-energy one, although the size dependence is weaker. The low-energy peak has commonly been observed for oxidized nc-Si, e.g., nc-Si embedded in SiO_2 matrices^{12,13,26} and surface-oxidized porous Si.^{27,28} This peak is assigned to the recombination of carriers trapped at P_b centers at nc-Si/ SiO_2 interfaces.²⁶

C. Time-resolved PL study

Figure 4 shows the temperature dependence of the PL decay curves for the sample with $d_{\text{av}}=9.0$ nm. The decay curves were monitored at the PL peak energy at 4 K (Table I). At 4 K, the decay curve is single-exponential, and the PL lifetime is 8.0 ms. With increasing temperature, the PL lifetime becomes shorter. In Fig. 5, the PL lifetime is plotted as a function of the temperature for the largest ($d_{\text{av}}=9.0$ nm) and the smallest ($d_{\text{av}}=4.2$ nm) nc-Si studied. We can see that the temperature dependence of the PL lifetime is much different between the two samples. For the sample with d_{av}

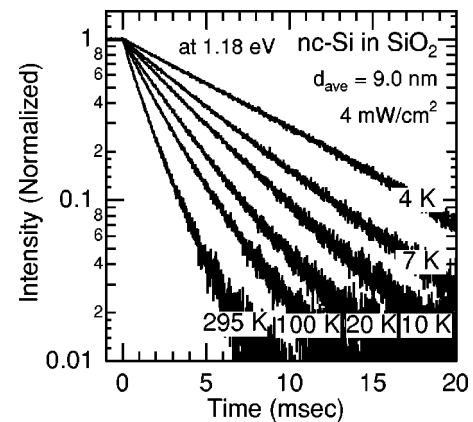


FIG. 4. Dependence of the PL decay curves on the temperature for $d_{\text{av}}=9.0$ nm. The decay curves were monitored at 1.18 eV.

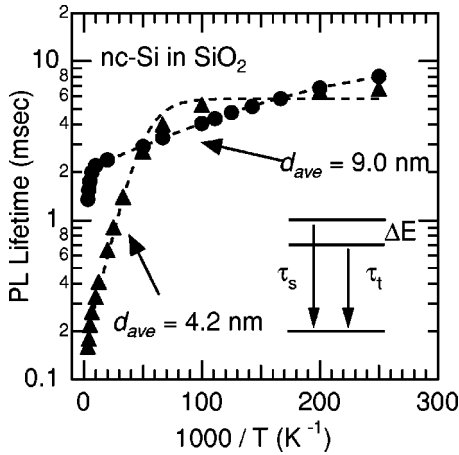


FIG. 5. Temperature dependence of the PL lifetime. The theoretical fit is shown by the broken curves.

=4.2 nm, the PL lifetime changes abruptly at 10–20 K. On the other hand, for $d_{av}=9.0$ nm, the PL lifetime gradually decreases until 150 K. With further increasing temperature, it decreases abruptly. Similar shortening of the PL lifetime above 150 K was observed for all the samples, and the mechanism will be discussed later.

In general, the PL lifetime (τ) is expressed as $\tau = \tau_r \tau_{nr} / (\tau_r + \tau_{nr})$, where τ_r and τ_{nr} are the radiative and nonradiative lifetime, respectively. Moreover, the PL intensity is proportional to $\tau_{nr} / (\tau_r + \tau_{nr})$.²⁵ In the present study, the PL intensity is almost independent of the temperature, which suggests that the observed PL lifetime reflects the radiative one for all the temperature range studied.

The temperature dependence of the PL lifetime for Si nanostructures is often well fitted by the model proposed by Calcott *et al.*^{9,10} In this model (see the inset of Fig. 5), the excitonic levels are split by energy (ΔE) due to the exchange interaction of an electron and a hole. The lower (upper) level is a triplet (singlet) state with a radiative lifetime τ_t (τ_s). The overall temperature dependence of the PL lifetime can be calculated on the basis of Boltzmann statistics with a weight factor of 3 for the triplet state and is described as

$$\frac{1}{\tau} = \frac{\frac{3}{\tau_t} + \frac{1}{\tau_s} \exp\left(-\frac{\Delta E}{k_B T}\right)}{3 + \exp\left(-\frac{\Delta E}{k_B T}\right)}, \quad (1)$$

where k_B and T are the Boltzmann constant and temperature, respectively. The broken curves in Fig. 5 represent the results of the fitting. We can see that this model can well reproduce the observed temperature dependence of the PL lifetime below 150 K.

In Fig. 6, the fitting parameters obtained (τ_s , τ_t , and ΔE) are plotted as a function of the PL energy. τ_s , τ_t , and ΔE for the present samples are plotted by solid circles, solid triangles, and solid diamonds, respectively. For comparison purposes, parameters reported for surface-oxidized porous Si (Refs. 9 and 10) and fresh porous Si (Ref. 5) are also plotted. The values of ΔE theoretically predicted for H-terminated nc-Si (Ref. 29) are shown by a solid curve. We can see that τ_s , τ_t , and ΔE for surface-oxidized nc-Si have strong PL

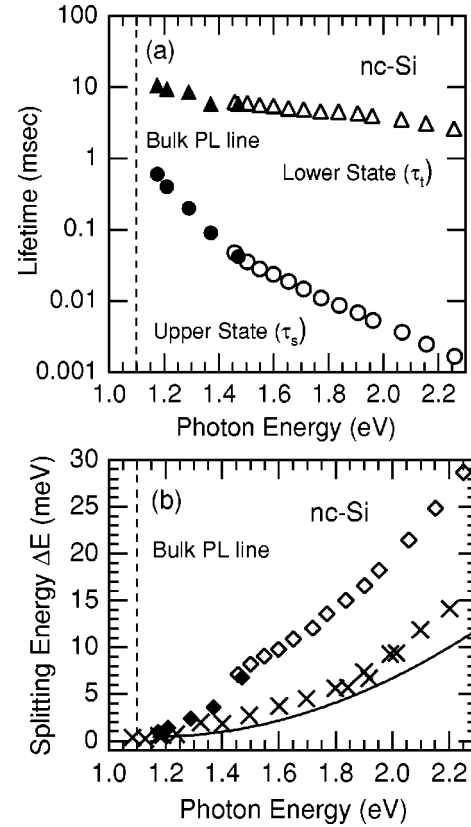


FIG. 6. (a) The lifetimes of the upper (τ_s) and lower (τ_t) excitonic states and (b) the exchange splitting energy (ΔE) as a function of the monitored PL energy. The solid circles, solid triangles, and solid diamonds correspond to the present results. The open circles, open triangles, and open diamonds represent the previous results for surface-oxidized porous Si (Refs. 9 and 10). The crosses are ΔE for fresh porous Si (Ref. 5). The solid curve represents the calculated ΔE for H-terminated nc-Si (Ref. 29).

energy dependence. As the PL energy increases, τ_s and τ_t become shorter and ΔE becomes larger. Furthermore, all these values change continuously in a very wide PL energy range, although the method of the sample preparation is different between the present samples and the previous ones.^{9,10} This indicates that the observed PL energy dependences are the intrinsic features of surface-oxidized nc-Si.

The values of τ_s , τ_t , and ΔE represent the degree of carrier confinement; τ_s and τ_t depend on the optical transition oscillator strength and ΔE is determined by the spatial separation between an electron and a hole in nc-Si. The continuous change of these parameters suggests that the PL mechanism is the same in the wide PL energy range. Furthermore, the PL peak energy and the splitting energy of excitons change continuously from the bulk values. This continuity from the bulk values indicates that the PL is due to the recombination of electron-hole pairs confined in nc-Si, i.e., a quantum confinement model.

Some authors have suggested that oxygen-related localized states (surface states) would contribute to the carrier recombination process because the size dependence of the PL properties is weak in the visible region.^{8,18–22} Recently, Wolkin *et al.*⁸ calculated the energy-band structure of O-terminated nc-Si and showed that, in nc-Si as small as a few nanometers in diameter, oxygen-related luminescent

centers locate in the band gap. The luminescent centers may contribute to the PL process, and thus PL properties in the visible region are almost independent of the size. On the other hand, their calculation suggests that for nc-Si larger than about 3 nm in diameter, PL originates from the recombination of electrons and holes in the conduction and valence bands, respectively, and the PL energy depends on the size. This theoretical prediction is really consistent with the present results. We can thus conclude that it is not necessary to take into account the contribution of surface states to the recombination process of electron-hole pairs in nc-Si in the size range studied in this work.

As shown in Fig. 6(b), ΔE of surface-oxidized nc-Si is larger than that of fresh porous Si and the theoretically predicted one. One possible explanation of the difference is that the shape of the confinement potential is different between surface-oxidized nc-Si and fresh porous Si. The surface of fresh porous Si is passivated by H atoms. The H termination forms abrupt potential barriers for excitons. On the other hand, in the case of surface-oxidized nc-Si, the SiO_x layer exists at the interfaces between nc-Si and SiO_2 matrices. The band gap of SiO_x changes depending on x and is generally much smaller than stoichiometric SiO_2 . As a result, the barrier has a gentle slope and exciton wave functions penetrate deep into the SiO_x layer. Thus, to achieve the same confinement energy, the size of surface-oxidized nc-Si should be smaller than that of fresh porous Si, resulting in the increase in the exchange splitting energy of excitons.

In Fig. 5, we can see that the temperature dependence of the PL lifetime deviates from the fitted line above 150 K. This discrepancy may be due to the oversimplification of the model, i.e., τ_s , τ_t , and ΔE are independent of temperature. Since the indirect gap nature is preserved for large nc-Si,^{6,30} at low temperatures, PL is assisted by the emission of momentum-conserving phonons, whereas at high temperatures, both emission and absorption processes become possible. The contribution of the phonon absorption process at high temperatures may lead to the modification of three parameters, resulting in the deviation of the temperature dependence from the model.

In Figs. 3 and 6, we demonstrated that the values of the PL peak energy and ΔE approach those of the bulk values with increasing size. Similarly, the other two parameters (τ_s and τ_t) are also considered to approach the bulk values. In bulk Si crystal, τ_s and τ_t are not experimentally obtained because the dominant carrier recombination process in bulk Si is the nonradiative one. The present results may allow us to estimate τ_s and τ_t of bulk Si crystal by extrapolating the PL energy dependence of τ_s and τ_t [Fig. 6(a)]. τ_s and τ_t at 1.10 eV, which is the bulk PL line with an emission of one momentum-conserving TO/LO phonon,⁵ are estimated to be 1.0 and 12 ms, respectively.

IV. CONCLUSION

We have demonstrated that the PL energy of surface-oxidized nc-Si can be tunable in a wide range from the vicinity of the bulk band gap to the visible region by just controlling the size. Furthermore, it was found that the PL lifetime and the exchange splitting energy of excitons in nc-Si have strong size dependence. These strong size dependences as well as the continuity from their bulk values indicate the quantum confinement model as the origin of the PL; it is not necessary to take into account the contribution of localized states to explain the observed PL properties of nc-Si in the size range studied in this work. We also demonstrated that the size of surface-oxidized nc-Si is smaller than that of porous Si at the same confinement energy. The different shapes of the potential barriers may be responsible for the observed difference in the PL properties.

ACKNOWLEDGMENTS

This work was supported by a Grant-in-Aid for Scientific Research from the Ministry of Education, Science, Sports and Culture, Japan, and a Grant for Research for the Future Program from the Japan Society for the Promotion of Science (JSPS-RFTF 96P-00305 and JSPS-RFTF-98P-01203). One of the authors (S.T.) would like to thank the Japan Society for the Promotion of Science for financial support.

*Author to whom correspondence should be addressed. Electronic mail: fujii@eedept.kobe-u.ac.jp

¹L.T. Canham, Appl. Phys. Lett. **57**, 1046 (1990).

²A.G. Cullis, L.T. Canham, and P.D.J. Calcott, J. Appl. Phys. **82**, 909 (1997).

³R.T. Collins, P.M. Fauchet, and M.A. Tischler, Phys. Today **50** (1), 24 (1997).

⁴*Light Emission in Silicon: From Physics to Devices*, edited by D. J. Lockwood (Academic Press, San Diego, 1998).

⁵D. Kovalev, H. Heckler, G. Polisski, and F. Koch, Phys. Status Solidi B **215**, 871 (1999).

⁶D. Kovalev, H. Heckler, M. Ben-Chorin, G. Polisski, M. Schwartzkopff, and F. Koch, Phys. Rev. Lett. **81**, 2803 (1998).

⁷G. Polisski, H. Heckler, D. Kovalev, M. Schwartzkopff, and F. Koch, Appl. Phys. Lett. **73**, 1107 (1998).

⁸M.V. Wolkin, J. Jorne, P.M. Fauchet, G. Allan, and C. Delerue, Phys. Rev. Lett. **82**, 197 (1999).

⁹P.D.J. Calcott, K.J. Nash, L.T. Canham, M.J. Kane, and D. Brumhead, J. Lumin. **57**, 257 (1993).

¹⁰P.D.J. Calcott, K.J. Nash, L.T. Canham, M.J. Kane, and D. Brumhead, J. Phys.: Condens. Matter **5**, L91 (1993).

¹¹Y. Kanzawa, T. Kageyama, S. Takeoka, M. Fujii, S. Hayashi, and K. Yamamoto, Solid State Commun. **102**, 533 (1997).

¹²M. Fujii, S. Hayashi, and K. Yamamoto, in *Recent Research Development in Applied Physics*, edited by S. G. Pandalai (Transworld Research Network, Trivandrum, 1998), Vol. 1, p. 193.

¹³M. Fujii, A. Mimura, S. Hayashi, and K. Yamamoto, Appl. Phys. Lett. **75**, 184 (1999).

¹⁴H. Takagi, H. Ogawa, Y. Yamazaki, A. Ishizaki, and T. Nakagiri, Appl. Phys. Lett. **56**, 2379 (1990).

¹⁵S. Schuppler, S.L. Friedman, M.A. Marcus, D.L. Adler, Y.-H. Xie, F.M. Ross, Y.J. Chabal, T.D. Harris, L.E. Brus, W.L. Brown, E.E. Chanban, P.F. Szajowski, S.B. Christman, and P.H. Citrin, Phys. Rev. B **52**, 4910 (1995).

¹⁶S. Guha, J. Appl. Phys. **84**, 5210 (1998).

¹⁷S. Guha, B. Qadri, R.G. Musket, M.A. Wall, and T. Shimizu-Iwayama, J. Appl. Phys. **88**, 3954 (2000).

¹⁸Y. Kanemitsu, T. Ogawa, K. Shiraishi, and K. Takeda, Phys. Rev. B **48**, 4883 (1993).

- ¹⁹R.E. Hummel, A. Morrone, M. Ludwig, and S.-S. Chang, *Appl. Phys. Lett.* **63**, 2771 (1993).
- ²⁰S.M. Prokes, W.E. Carlos, and O.J. Glembocki, *Phys. Rev. B* **50**, 17 093 (1994).
- ²¹Y. Kanemitsu, S. Okamoto, M. Otobe, and S. Oda, *Phys. Rev. B* **55**, R7375 (1997).
- ²²K.S. Zhuravlev, A.M. Gilinsky, and A.Yu. Kobitsky, *Appl. Phys. Lett.* **73**, 2962 (1998).
- ²³M.S. Brandt, H.D. Fuchs, M. Stutzmann, J. Weber, and M. Cardona, *Solid State Commun.* **81**, 307 (1992).
- ²⁴P.G. Pai, S.S. Chao, Y. Takagi, and G. Lucovsky, *J. Vac. Sci. Technol. A* **4**, 689 (1986).
- ²⁵J.C. Vial, A. Bsiesy, F. Gaspard, H. Hérino, M. Ligeon, F. Muller, R. Romestain, and R.M. Macfarlane, *Phys. Rev. B* **45**, 14 171 (1992).
- ²⁶M. Fujii, A. Mimura, S. Hayashi, K. Yamamoto, C. Urakawa, and H. Ohta, *J. Appl. Phys.* **87**, 1855 (2000).
- ²⁷G. Mauckner, J. Hamann, W. Rebitzer, T. Baier, K. Thonke, and R. Sauer, in *Microcrystalline and Nanocrystalline Semiconductors*, edited by L. Brus, M. Hirose, R.W. Collins, F. Koch, and C.C. Tsai, Mater. Res. Soc. Symp. Proc. 358 (Materials Research Society, Pittsburgh, 1995), 489.
- ²⁸V. Petrova-Koch, T. Muschik, G. Polisski, and D. Kovalev, in *Microcrystalline and Nanocrystalline Semiconductors* (Ref. 27), 483.
- ²⁹F.A. Reboredo, A. Franceschetti, and A. Zunger, *Appl. Phys. Lett.* **75**, 2972 (1999).
- ³⁰M.S. Hybertsen, *Phys. Rev. Lett.* **72**, 1514 (1994).